metals

MDPI

Article

Investigation of Carbothermic Reduction of Ilmenite Concentrate with Calcium Carbonate Addition Using the Rietveld Method

Xiaoli Wang [1,2], Yang Li [1], Huajun Wang [1], Chunbao Sun [1] and Jue Kou [1,*]

[1] School of Civil and Resources Engineering, University of Science and Technology Beijing, Beijing 100083, China; xiaoliwang@ustb.edu.cn (X.W.); d202210037@xs.ustb.edu.cn (Y.L.); wanghj@ustb.edu.cn (H.W.); suncb@ustb.edu.cn (C.S.)

[2] State Key Laboratory of Mineral Processing, Beijing 100160, China

* Correspondence: koujue@ustb.edu.cn

Abstract: The carbothermic reduction of ilmenite concentrate was performed with the addition of calcium carbonate ($CaCO_3$) as an additive. The effects of roasting temperature and $CaCO_3$ content on calcium titanate ($CaTiO_3$) formation and metallic iron reduction were investigated. The Rietveld method was employed for qualitative and quantitative analysis of roasting products. It was found that as the temperature increased from 1000 °C to 1400 °C, the calcium titanate content increased from 21.95% to 83.02%. Similarly, as the $CaCO_3$ content increased, the calcium titanate content rose from 0% to 83.11%, while the metallic iron content increased from 4.52% to 10.37%. SEM-EDS analysis suggested that adding $CaCO_3$ during the carbothermic reduction of ilmenite promoted the aggregation and growth of metallic iron particles. The roasting products obtained under optimal conditions were subjected to three-stage grinding and three-stage magnetic separation. The final metallic iron product had a grade of 90.01% and a recovery rate of 91.32%. The calcium titanate product contained 55.43% TiO_2, with a titanium recovery rate of 85.90%. Rietveld results indicated that the calcium titanate product had a high purity, with a content of 90.87%. This study effectively improved the comprehensive utilization of titanium and iron resources in ilmenite.

Keywords: ilmenite; carbothermic reduction; calcium titanate; calcium carbonate; Rietveld method

check for updates

Citation: Wang, X.; Li, Y.; Wang, H.; Sun, C.; Kou, J. Investigation of Carbothermic Reduction of Ilmenite Concentrate with Calcium Carbonate Addition Using the Rietveld Method. *Metals* **2024**, *14*, 1321. https://doi.org/10.3390/met14121321

Academic Editor: Antoni Roca

Received: 25 October 2024
Revised: 16 November 2024
Accepted: 19 November 2024
Published: 22 November 2024

1. Introduction

Calcium titanate is a typical material with perovskite structure [1]. Due to its excellent dielectric properties, such as low dielectric loss and high dielectric constant [2,3], it is widely used in ceramics, catalytic tubes, display, and storage devices [4–6]. Additionally, its conductivity and polarity make it widely applicable in biomedical fields [7,8] and its photocatalytic application in advanced oxidation processes (AOPs) [9,10]. The synthesis methods of calcium titanate mainly include the conventional solid-state reaction method, molten salt synthesis, mechanical synthesis, sol–gel method, and hydrothermal synthesis [11–13]. However, these methods generally involve long reaction times, complex procedures, and high energy consumption and may lead to serious environmental contamination [14,15]. Therefore, it is necessary to find an environmentally friendly and low-cost alternative process for the preparation of calcium titanate.

Ilmenite ($FeTiO_3$) is one of the most important titanium-bearing minerals, primarily composed of iron oxide and titanium oxide. It is extensively utilized in various fields such as aerospace, healthcare, chemical engineering, and machinery manufacturing [16,17]. The carbothermic reduction is a well-established method for the treatment of ilmenite and has become one of the important methods for developing and utilizing ilmenite resources due to its simplicity of operation and short process [18–20]. In this method, iron is reduced to metallic iron, while titanium remains in the form of oxides. The titanium and iron resources can be separated through grinding and magnetic separation. However, the titanium slag obtained through this method has a high impurity content and cannot be directly used as a raw material for producing titanium dioxide, leading to inefficient utilization of titanium resources [21,22].

Recent research demonstrated that the addition of calcium, magnesium, or sodium compounds in the direct reduction process of vanadium–titanium magnetite allows for the conversion of titanium into calcium titanate or magnesium titanate [23–26]. Li et al. investigated the effect of calcium compounds on the carbothermic reduction of vanadium–titanium magnetite concentrate and concluded that calcium compounds can improve the metallization rate of the reduced products [27]. Chen et al. found that adding magnesium oxide during the carbothermic reduction process of vanadium–titanium magnetite promotes the reduction of metallic iron [28]. Yu et al. conducted a direct carbothermic reduction of ilmenite concentrates using a high dose of Na_2CO_3 in a microwave field. They found that the addition of Na_2CO_3 significantly reduced the reduction temperature and time, promoting the reduction of metallic iron [29]. It can be concluded that calcium or magnesium compounds have a significant impact on the carbothermic reduction of ilmenite. However, previous studies did not specifically quantify the reduction roasting products but rather made judgments based on the intensity of diffraction peaks, lacking strong evidence to confirm the promoting effect of calcium or magnesium compounds on the direct reduction roasting process. The Rietveld method [30] is an effective technique for conducting quantitative phase analysis. However, the application of the Rietveld method in the analysis of roasting products has been explored in only a few studies.

This study focuses on the carbothermic reduction of ilmenite concentrate using bituminous coal as a reductant and calcium carbonate ($CaCO_3$) as an additive. The formation mechanism of calcium titanate is studied through thermodynamic analysis, X-ray diffraction (XRD), and scanning electron microscopy–energy dispersive spectroscopy (SEM-EDS). Furthermore, the effects of roasting temperature and calcium carbonate content on calcium titanate production are also investigated. The Rietveld method is used for qualitative and quantitative analysis of the raw materials and roasted products. This technique enables precise quantification of phase transformations, offering insights into the impact of roasting temperature and calcium carbonate addition on the formation of calcium titanate and metallic iron. This study aims to enhance the comprehensive utilization efficiency of titanium and iron resources in ilmenite.

2. Materials and Methods

2.1. Materials

The ilmenite concentrate used in this study was collected from Panxi, Sichuang Province, China. It was obtained from the tailings of vanadium–titanium magnetite after iron selection through strong magnetic separation and flotation. The main chemical compositions of ilmenite concentrate are presented in Table 1. The contents of TiO_2 and Fe_2O_3 were 43.77% and 51.41%, respectively. The phase contents of ilmenite concentrate were determined by the Rietveld method. The result is shown in Figure 1 and Table 2. According to the results, the measured patterns showed a good agreement with calculated patterns. The R_{wp} value was 6.62%, which indicated high reliability of the results. The ilmenite (PDF: 01-075-1203) content of the sample was 86.13%. Moreover, there were several other minerals, including the following: forsterite (PDF: 97-000-0686) (3.01%), diopside (PDF: 01-071-6477) (2.52%), chlorite (PDF: 01-075-8295) (2.75%), magnetite (PDF: 01-071-4918) (1.45%), hornblende (PDF: 01-073-3984) (1.18%), quartz (PDF: 01-070-2516) (1.25%), and traces of anatase (PDF: 01-070-6826) (0.82%) and plagioclase (PDF: 01-073-9850) 0.79%. The particle size composition of the sample is shown in Figure 2. It can be seen that the particle size of less than 0.074 mm accounts for 80.48%.

Table 1. Main chemical compositions of ilmenite concentrate.

	TiO_2	Fe_2O_3	MnO	SiO_2	CaO	MgO	Al_2O_3	P_2O_5	Na_2O	SO_3
Content wt. %	43.77	51.41	1.06	0.97	0.72	0.69	0.62	0.42	0.10	0.09

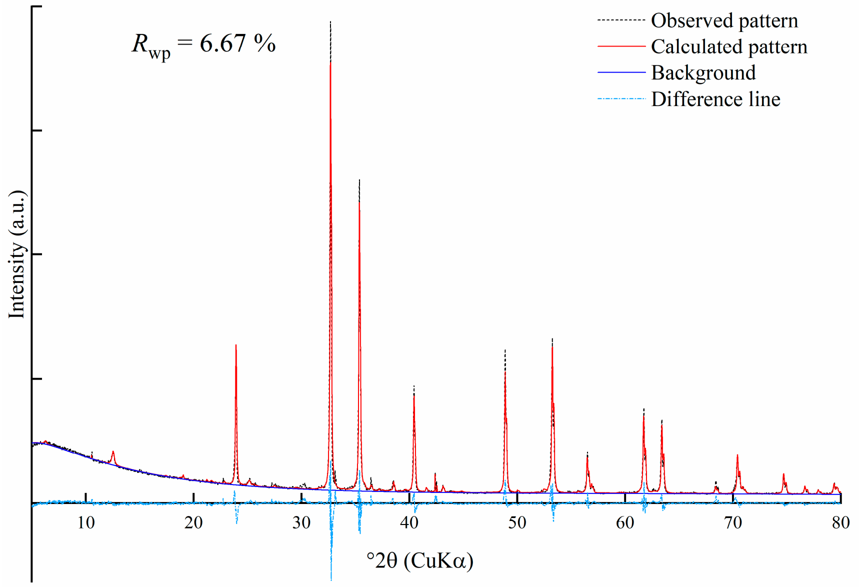

Figure 1. Rietveld refinement result of ilmenite concentrate sample.

Table 2. Quantitative results of sample by Rietveld method.

Mineral Phase	**R_{wp} = 6.62%**								
	Ilmenite	**Forsterite**	**Diopside**	**Chlorite**	**Magnetite**	**Hornblende**	**Quartz**	**Anatase**	**Plagioclase**
wt.%	86.13 (5) *	3.01 (3)	2.52 (2)	2.75 (1)	1.45 (1)	1.18 (3)	1.25 (1)	0.82 (1)	0.79 (2)

*: the standard deviation.

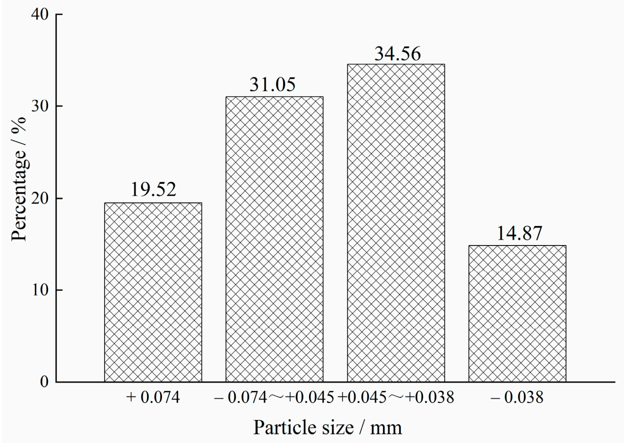

Figure 2. Particle size composition of sample.

The reducing agent used in this study is bituminous coal from Sichuan Province, China, which was crushed to a particle size of less than 2 mm. The industrial analysis of the bituminous coal was performed, and the results are shown in Table 3. The contents of fixed carbon, volatile ash, and moisture were 62.24%, 30.92%, 4.69%, and 2.15%, respectively. The additive used in the experiment was analytically pure calcium carbonate ($CaCO_3$), which was purchased from Sinopharm Chemical Reagent Co., Ltd., Shanghai, China.

Table 3. Industrial analysis of bituminous coal.

	Fixed Carbon/%	**Volatile/%**	**Ash/%**	**Moisture/%**
Bituminous coal	62.24	30.92	4.69	2.15

2.2. Methods

2.2.1. Experiment Procedures

Figure 3 presents the flow diagram of the direct carbothermic reduction and magnetic separation process of ilmenite concentrate using calcium carbonate as an additive, which is mainly divided into the following three sections:

(1) Pelletizing: 100 g of ilmenite concentrate was mixed with a certain amount of calcium carbonate in a certain proportion, and then an appropriate amount of water was added and mixed to form pellets with a diameter of 8~10 mm. The pellets were placed in a constant-temperature drying oven at 105 °C and dried for 4 h.

(2) Reduction roasting: Three pellets were placed in a graphite crucible, which was then filled with varying amounts of bituminous coal to fully embed the pellets, ensuring an adequate reducing atmosphere. The muffle furnace was heated at a rate of 10 °C/min. Once the target temperature was reached, the graphite crucible was placed in the muffle furnace. After roasting for 3 h, the crucible was removed and cooled at room temperature to obtain roasted pellets.

(3) Magnetic separation: After cooling, the roasted pellets were crushed to less than 2 mm. The crushed products were then subjected to a three-stage grinding and three-stage magnetic separation process. The grinding was performed using a three-roller, multi-cylinder rod mill, operating at a grinding concentration of 67% and a rotational speed of 289 rpm. The magnetic separation intensities were set as follows: 263 kA/m for the first stage, 95 kA/m for the second stage, and 80 kA/m for the third stage. The non-magnetic product obtained from the first stage of magnetic separation was calcium titanate, while the magnetic product obtained from the third stage was reduced iron. The non-magnetic product obtained in the second stage is an intermediate product.

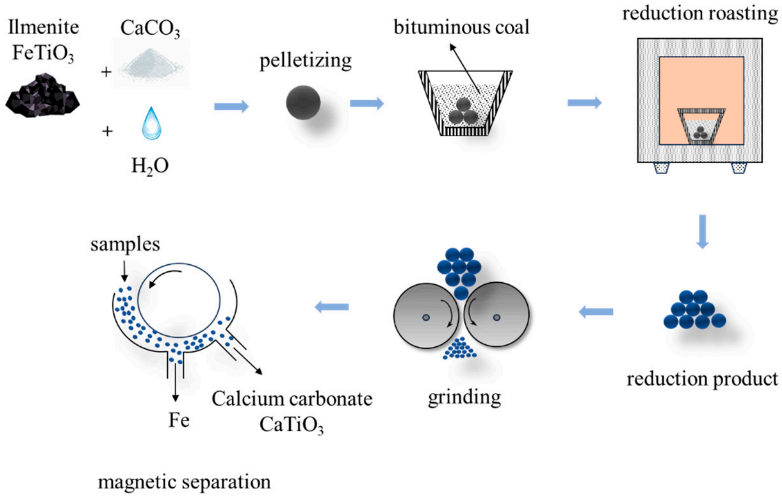

Figure 3. Flow diagram of the carbothermal reduction and magnetic separation process of ilmenite.

2.2.2. Rietveld Method

The Rietveld method was employed to determine the types and contents of reduction products and the phase transition process in this study. This method minimizes the difference between calculated and measured XRD patterns by the least squares approach (Equation (1)) and extracts crystal structure information from patterns [31]. The weighted profile R factor (R_{wp}) is one of the indicators used to evaluate the Rietveld refinement results (Equation (2)). Generally, the smaller the R_{wp} value, the better the pattern fit and the higher the reliability of the result.

$$\sum_i w_i (y_{io} - y_{ic})^2 = Minimum \tag{1}$$

$$R_{wp} = \sqrt{\frac{\sum w_i (y_{io} - y_{ic})^2}{\sum w_i \, {y_{io}}^2}} \tag{2}$$

where y_{io} and y_{ic} are observed and calculated intensities at point i, and w_i is the weight assigned to each intensity.

The program BGMN was used for the Rietveld refinement, which includes an extensive database of common minerals and compounds crystal structure models [32,33]. BGMN also supports adding additional crystal structure models via CIF files from the Inorganic Crystal Structure Database (ICSD) [34] and the COD Crystallography Open Database [35]. During the refinement, the lattice parameters, scaling factor, and peak broadening parameters and the parameter of preferred orientation correction were refined. The zero point shift correction and the sample displacement error were refined as non-structural parameters. The initial structural models of calcium titanate, iron and ferropseudobrookite during the refinement are provided in the Supplementary Materials.

2.2.3. Analytical Methods

The X-ray powder diffraction measurements were performed on a D8 Advance diffractometer (Bruker, Karlsruhe, Germany) with Cu Kα radiation (λ = 0.1542 nm) operating at 40 kV and 40 mA. The scanning angle 2θ ranged from 5° to 80° with a step size of 0.04°. The microstructure of the sample was investigated by scanning electron microscopy–energy dispersive spectrometer (SEM-EDS) using a SUPRA 55 field emission-scanning electron microscope equipped with a LinkNA1000 energy spectrometer (Zeiss, Oberkochen, Germany).

3. Results and Discussion

3.1. Effect of Temperature on Mineral Phase Transformation During the Carbothermic Process

To investigate the effect of roasting temperature on the formation of calcium titanate, the mineral phase transformation was analyzed within the temperature range of 1000 °C to 1500 °C under conditions of 60 w.t.% $CaCO_3$ addition and a reduction time of 120 min. The XRD patterns of reduction products at different roasting temperatures are shown in Figure 4. The results indicated that the roasting temperature greatly affects the phase composition of direct reduction roasted products. At a temperature of 1000 °C, the primary reduction products are CaO (PDF: 01-070-5490), calcium titanate (PDF: 01-070-7337), and iron (01-071-3763), suggesting that only a limited amount of ilmenite reacts with $CaCO_3$ to form calcium titanate at this temperature. With increasing temperature, the diffraction peak intensity of calcium titanate progressively increased, while the intensity of the CaO diffraction peak sharply declined (Figure 4).

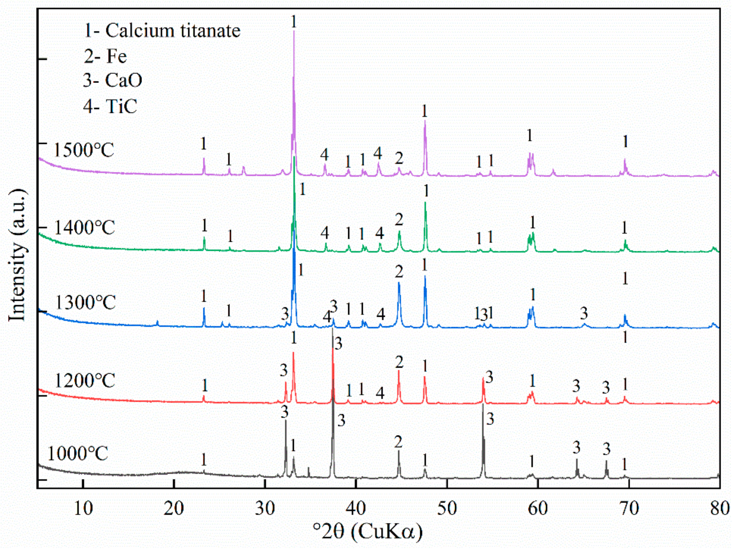

Figure 4. Effect of roasting temperature on phase transformation of roasted products.

Table 4 presents the results of the Rietveld refinement, which reflect the changes in the content of the roasted products. The refined results of the lattice parameters for calcium titanate, iron, and ferropseudobrookite are detailed in the Supplementary Materials. Figure 5 illustrates the trend of the calcium titanate, CaO, and iron content in the reduction products as the temperature varied. As the temperature increased, the calcium titanate content rose from 21.95% at 1000 °C to 83.02% at 1400 °C, while the CaO content decreased from 67.77% at 1000 °C to 0% at 1500 °C. It was evident that the rise in roasting temperature promoted the formation of calcium titanate. The Fe content increased from 7.34% at 1000 °C to 10.86% at 1300 °C and then decreased to 5.88% at 1500 °C (Figure 5). Therefore, the optimal roasting temperature is 1400 °C. This conclusion is consistent with the study of Li et al. [36]. They investigated the formation of calcium titanate during the carbothermal reduction of vanadium titanomagnetite concentrate with the addition of $CaCO_3$. It was found that at a specific amount of $CaCO_3$, the XRD diffraction peak of calcium titanate was strongest when the roasting temperature reached 1400 °C. This suggested that 1400 °C is optimal for the formation of calcium titanate.

Table 4. The Rietveld refinement results of roasted products at different temperatures (wt.%).

		Temperature/°C				
		1000	**1200**	**1300**	**1400**	**1500**
R_{wp}		11.90	11.16	10.98	11.47	10.53
Calcium titanate	$CaTiO_3$	21.95 (3) *	55.53 (3)	76.83 (3)	83.02 (3)	81.76 (5)
iron	Fe	7.34 (2)	9.57 (1)	10.86 (1)	9.35 (8)	5.88 (8)
CaO	CaO	67.77 (5)	30.44 (2)	2.96 (8)	-	-
Ferropseudobrookite	$FeTi_2O_5$	-	0.45 (3)	3.40 (3)	0.96 (2)	2.28 (5)
Ferrosilite	$FeSiO_3$	1.88 (4)	1.49 (2)	1.38 (2)	2.03 (2)	3.08 (3)
TiC	TiC		0.6 (1)	2.32 (1)	4.07 (1)	6.39 (2)
Armalcolite	$(Mg,Fe^{2+})Ti_2O_5$	-	0.3 (2)	0.45 (1)	0.57 (2)	0.62 (3)
Magnetite	Fe_3O_4	1.06 (1)	1.63 (8)	1.81 (7)	-	-

*: the standard deviation.

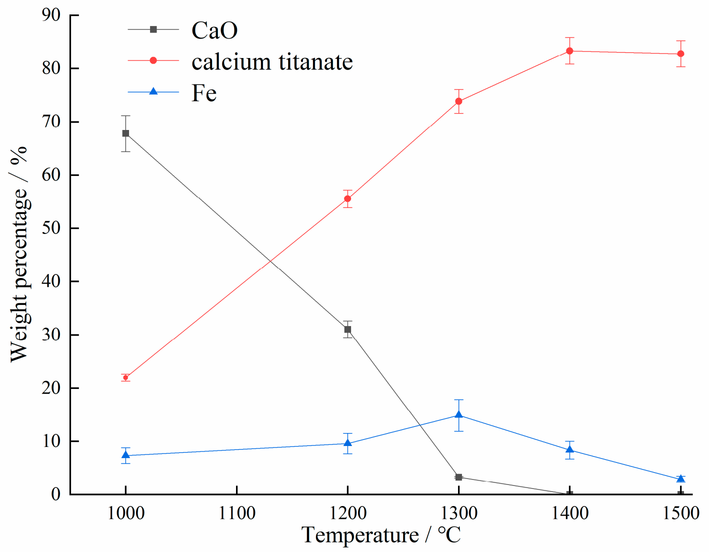

Figure 5. Variation of calcium titanate, CaO, and Fe content in roasted products with temperature.

Rietveld analysis revealed that the ilmenite concentrate contained small amounts of silicate minerals such as chlorite, diopside, and hornblende, which were converted into ferrosilite after roasting (Table 2). The content of ferrosilite (PDF: 01-076-0886) increased with the rise in roasting temperature (Table 4). Additionally, a small amount of TiC (PDF: 01-070-7697) was observed to form with the rise in temperature.

3.2. Effect of Calcium Carbonate Dosage on Mineral Phase Transformation During the Carbothermic Process

The effect of calcium carbonate ($CaCO_3$) content (0%, 20%, 40%, 50%, 60%, and 70%) on the formation of calcium titanate ($CaTiO_3$) was investigated under the conditions of a roasting temperature of 1400 °C, 60 w.t.% bituminous coal, and a roasting time of 120 min. As shown in Figure 6, the variation in $CaCO_3$ content affected the phase transformation of Fe and Ti in the roasting products. In the absence of $CaCO_3$, the direct reduction products were mainly composed of Fe and ferropseudobrookite ($FeTi_2O_5$) (PDF: 01-076-2372). However, when $CaCO_3$ was added, the main reduction products consisted of Fe, ferropseudobrookite, and calcium titanate. As the amount of $CaCO_3$ increased, the diffraction peak intensity of ferropseudobrookite in the reduction products continuously decreased, while the diffraction peak intensity of calcium titanate steadily increased (Figure 6).

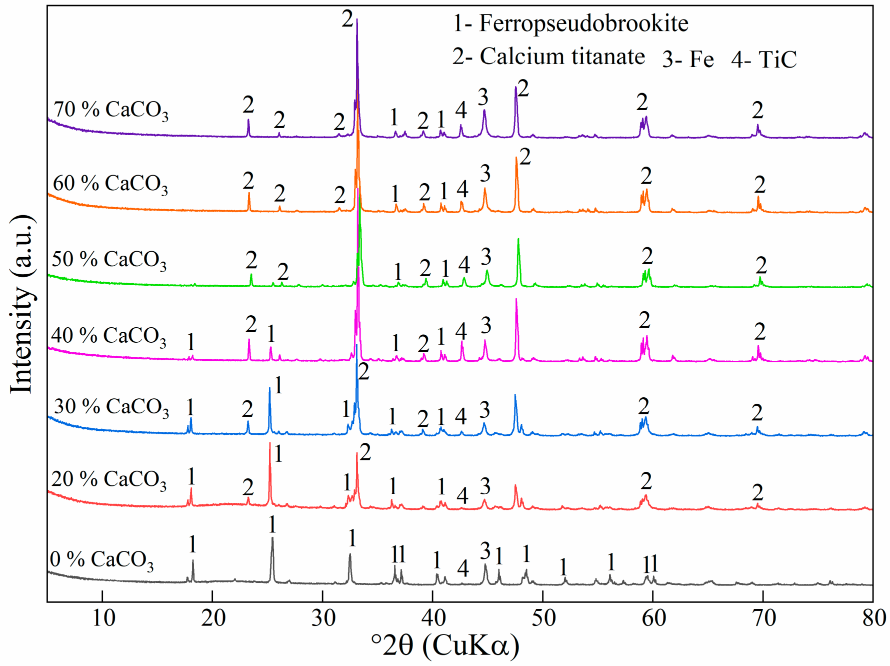

Figure 6. Variation of calcium titanate, CaO, and Fe content in the roasted products with increasing $CaCO_3$ content.

Rietveld results showed a significant change in the phase content of the roasted products (Table 5). The refined results of the lattice parameters for calcium titanate, iron, and ferropseudobrookite are detailed in the Supplementary Materials. Without the addition of $CaCO_3$, the reduction roasting products were primarily ferropseudobrookite (89.48%), and no calcium titanate was formed. With the addition of $CaCO_3$, calcium titanate was formed, and its content increased with the amount of $CaCO_3$, rising from 0% to 83.11% (Table 5). Additionally, as the $CaCO_3$ content increased, the metallic iron content rose from 4.52% to 10.37%, indicating that the addition of $CaCO_3$ can promote the reduction of ilmenite to metallic iron. In contrast, as the amount of $CaCO_3$ increased, the ferropseudobrookite content decreased from 89.48% to 1.01% (Table 5 and Figure 6).

Figure 7 shows the trend of calcium titanate, ferropseudobrookite, and iron content in the reduction products as the amount of $CaCO_3$ varies. The results indicated that $CaCO_3$ reacted with ilmenite to form calcium titanate, and when $CaCO_3$ was insufficient, ilmenite primarily converted into ferropseudobrookite. The optimal amount of $CaCO_3$ is 60 w.t.%. The Rietveld refinement results also showed that a small amount of ferrosilite and TiC was produced in the roasted product, which was consistent with previous research result (Table 4).

Table 5. The Rietveld results of roasted products with different amounts of calcium carbonate (wt.%).

		$CaCO_3$						
		0	**20**	**30**	**40**	**50**	**60**	**70**
R_{wp}		11.43	10.77	10.33	12.81	12.53	11.92	11.93
Calcium titanate	$CaTiO_3$	-	51.42 (4)	64.51 (2)	77.13 (5)	79.92 (3)	83.11 (3)	81.37 (3)
iron	Fe	4.52 (2)*	4.41 (1)	4.36 (1)	6.3 (1)	7.14 (1)	8.22 (1)	10.37 (1)
Ferropseudobrookite	$FeTi_2O_5$	89.48 (5)	41.83 (8)	28.93 (8)	8.29 (7)	4.51 (8)	1.01 (3)	1.79 (7)
Ferrosilite	$FeSiO_3$	2.39 (4)	1.12 (3)	1.0 (2)	4.19 (3)	4.22 (5)	2.53 (2)	2.03 (2)
TiC	TiC	1.61 (2)	1.28 (1)	1.19 (1)	4.09 (1)	4.21 (1)	5.12 (1)	4.44 (1)

*: the standard deviation.

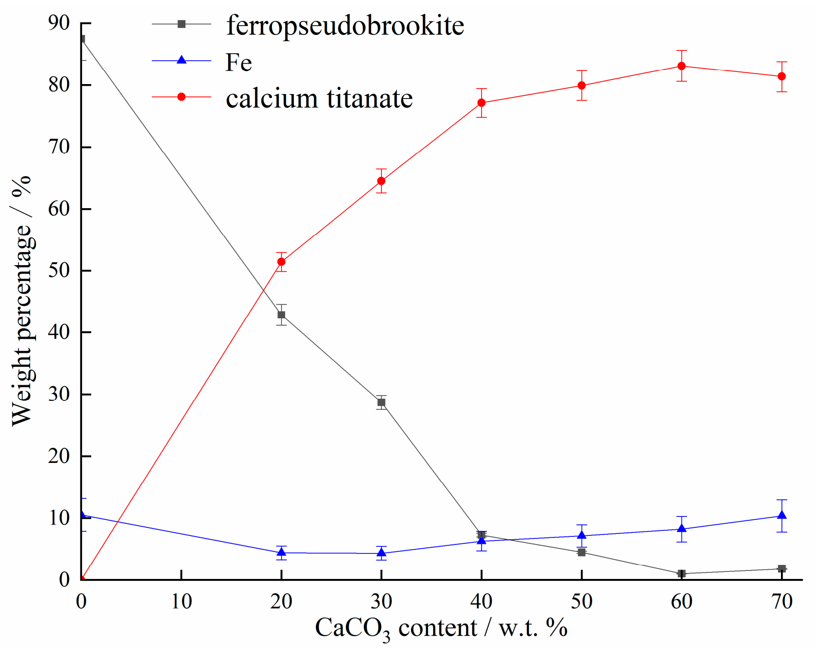

Figure 7. Variation of calcium titanate, ferropseudobrookite, and Fe content in the roasted products with $CaCO_3$ content.

3.3. Thermodynamic Analysis of Ilmenite Direct Reduction

The carbothermic reduction reaction of ilmenite is a complex process, involving a series of intermediate reactions. Thermodynamic analysis was conducted on the reduction process of ilmenite with the addition of calcium carbonate. The possible reactions occurring in the reduction system are shown in Equations (3)–(8). Thermodynamic calculations of the main reactions in the direct carbothermic reduction process of ilmenite were carried out using Factsage software (version 8.3), and the relationship between the standard Gibbs free energy ($\Delta_r G^\theta$) of each reaction and temperature was obtained. The results are shown in Figure 8.

$$C(s) + CO_2(g) \rightarrow 2CO(g) \tag{3}$$

$$CaCO_3(s) \rightarrow CaO(s) + CO_2(g) \tag{4}$$

$$2FeTiO_3(s) + CO(g) \rightarrow FeTi_2O_5(s) + Fe(s) + CO_2(g) \tag{5}$$

$$FeTiO_3(s) + CaCO_3(s) + CO(g) \rightarrow CaTiO_3(s) + Fe(s) + CO_2(g) \tag{6}$$

$$FeTiO_3(s) + CaO(s) + C(s) \rightarrow CaTiO_3(s) + Fe(s) + CO(g) \tag{7}$$

$$FeTiO_3(s) + 4C(s) \rightarrow TiC(s) + Fe(s) + 3CO(g) \tag{8}$$

As shown in Figure 8, calcium carbonate undergoes a decomposition reaction (Equation (4)) at around 850 °C. Reaction (5) can proceed spontaneously at a temperature above 1100 °C, as the value of $\Delta_r G^\theta$ is less than zero beyond this temperature. Equations (6) and (7) are easier to occur than Equation (5), as Equation (6) can spontaneously proceed at approximately 400 °C ($\Delta_r G^\theta < 0$) and Equation (5) at around 300 °C ($\Delta_r G^\theta < 0$). It can be concluded that the addition of calcium carbonate can promote the direct reduction of ilmenite, lower the reduction temperature, and make the reduction of ilmenite to metallic iron easier. Moreover, it can be observed that with the addition of calcium carbonate, titanium is present in the reduction products as calcium titanate ($CaTiO_3$), whereas without the addition of calcium carbonate, titanium is present in the form of ferropseudobrookite ($FeTi_2O_5$) in the reduction products. This conclusion is consistent with the previous XRD analysis results (Table 5). And the content of calcium titanate in the roasted products increased as the roasting temperature rose.

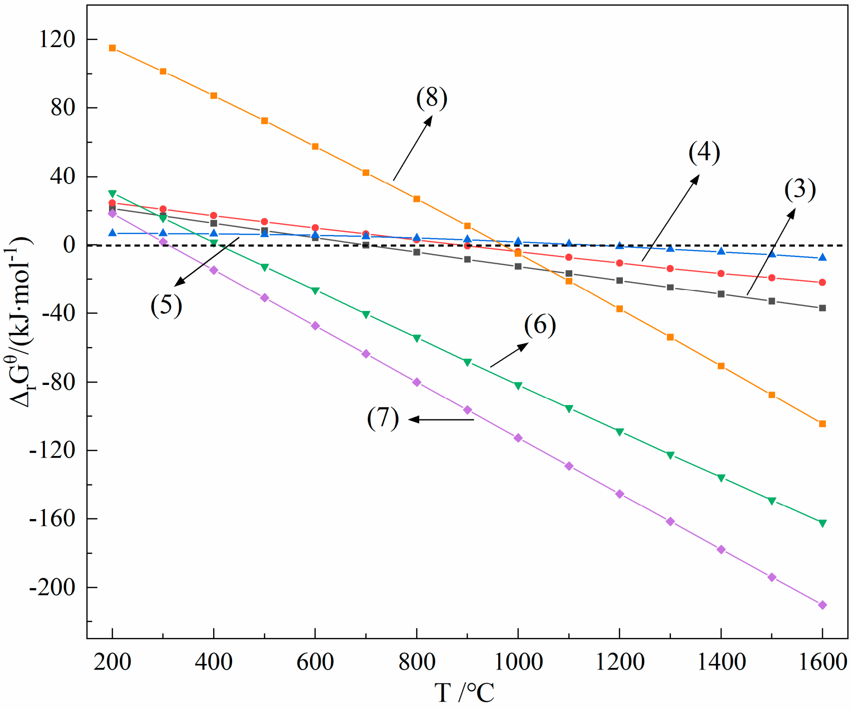

Figure 8. The relationship between $\Delta_r G^\theta$ and T in the carbothermic reduction process.

Equation (8) cannot proceed spontaneously below approximately 950 °C, as its $\Delta_r G^\theta$ value is greater than zero within this temperature range. However, when the temperature exceeds 950 °C, the reaction can occur spontaneously. Rietveld analysis showed that TiC formed at a roasting temperature of 1200 °C, and as the temperature increased, the TiC content rose from 0.6% to 6.39%. This indicated that a higher temperature was required for TiC formation in the actual reaction, which also promoted its formation.

3.4. Morphology of Roasted Products

SEM-EDS analysis was conducted on the roasted products under the optimal calcination conditions: 60 w.t.% $CaCO_3$, reduction temperature of 1400 °C, and reduction time of 120 min. The results are shown in Figure 9. The EDS analysis indicated that the brighter particles (point 1) corresponded to metallic iron, whereas the darker particles (point 2) were identified as calcium titanate. The SEM results indicated that under the optimal roasting conditions, large metallic iron particles formed in the reduction products, with particle sizes reaching approximately 100 µm. It was evident that the addition of $CaCO_3$ in the carbothermic reduction of ilmenite can promote the aggregation and growth of metallic iron particles. Additionally, the separation between metallic iron and calcium titanate was distinct and with large particles and clear boundaries, which were beneficial for the subsequent magnetic separation. Furthermore, the energy spectrum analysis in Figure 9 reveals that the reduction products contain only the constituent elements of the metallic iron and calcium titanate particles, with no impurity elements detected, indicating that the purity of these two reduction particles is high.

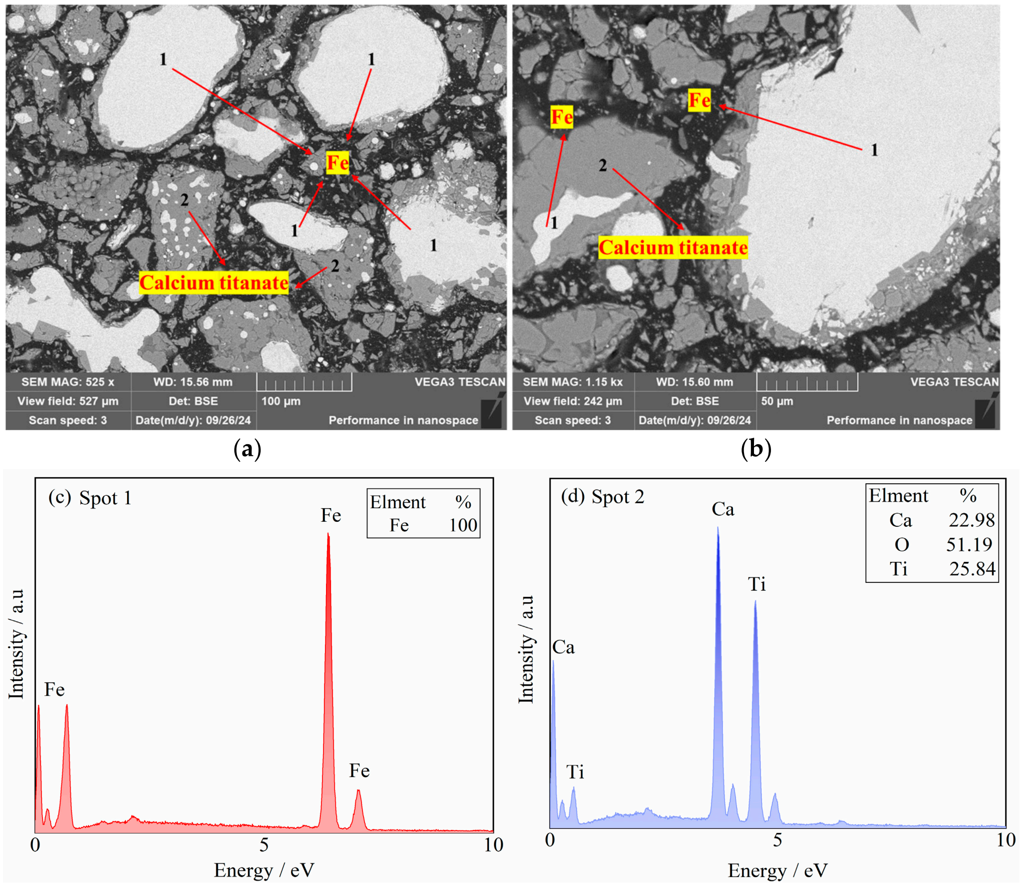

(**a**) (**b**)

Figure 9. SEM and EDS analysis of roasted products under optimal conditions: (**a**,**b**) SEM image; (**c**,**d**) EDS analysis.

3.5. Magnetic Separation of Calcium Titanate and Metallic Iron

The roasted products obtained under the optimal roasting conditions were subjected to grinding and magnetic separation to obtain metallic iron and calcium titanate products. Figure 10 presents the flowchart of magnetic separation indexes for roasted products. The first stage primarily recovers calcium titanate, while the second and third stages concentrate and recover reduced iron. The reduced iron product obtained from the first stage had a low iron grade, but the calcium titanate product achieved a higher grade and recovery rate (Figure 10). Therefore, the calcium titanate product was separated in the first-stage grinding and magnetic separation, while the reduced iron product from the first stage was re-ground and further separated to achieve a higher-grade reduced iron product. The reduced iron product obtained after the final magnetic separation with a total iron grade of 90.01% and a recovery rate of 91.321%. The calcium titanate product contained 55.43% TiO_2, with a titanium recovery rate of 85.90%.

Figure 11 presents the XRD analysis results of reduced iron and calcium titanate products after magnetic separation. Table 6 shows the Rietveld analysis results of the concentrate and tailings from the roasted products after magnetic separation. The results indicated that after magnetic separation of the roasted products, the main phase in the tailings was calcium titanate with a content of 90.87%, accompanied by a small amount of metallic iron at approximately 4.78%. The concentrate was composed primarily of metallic iron, with a content of 78.05%, and also contained 16.58% calcium titanate. Additionally, the concentrate and tailings contained a small amount of TiC, 3.19% and 1.35%, respectively. This result is consistent with the previous XRD analysis of the roasted products, demonstrating that grinding and magnetic separation can effectively separate metallic iron from calcium titanate, yielding calcium titanate with relatively high purity.

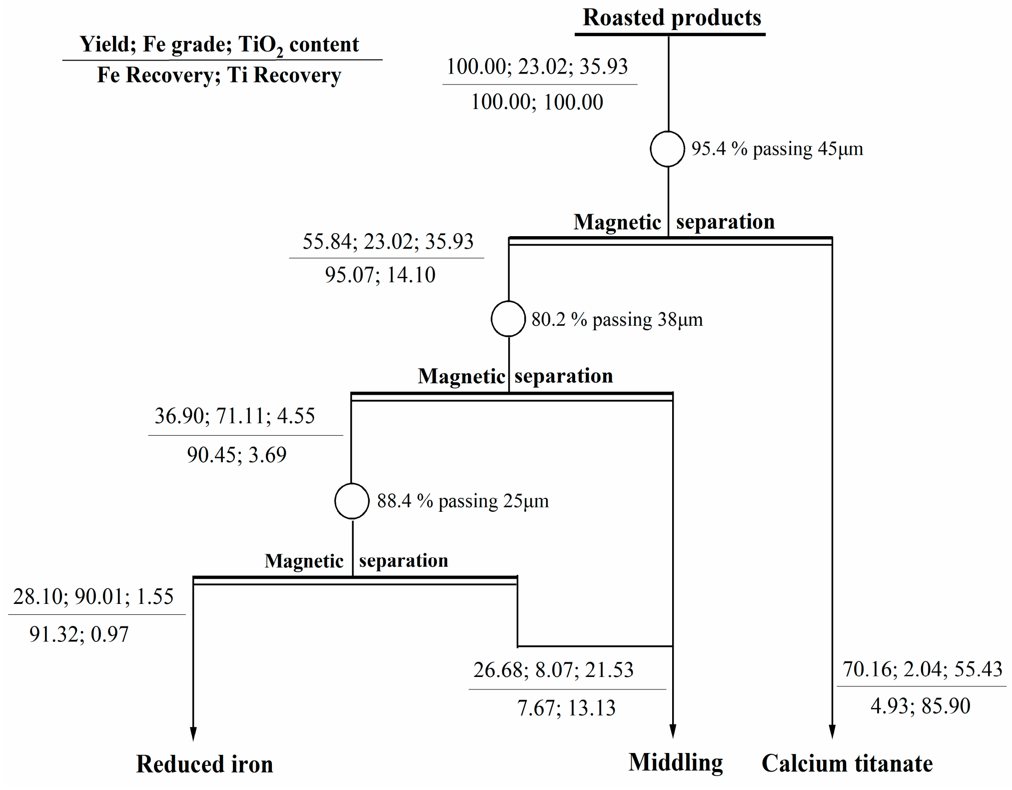

Figure 10. Flowchart of magnetic separation indexes for roasted products.

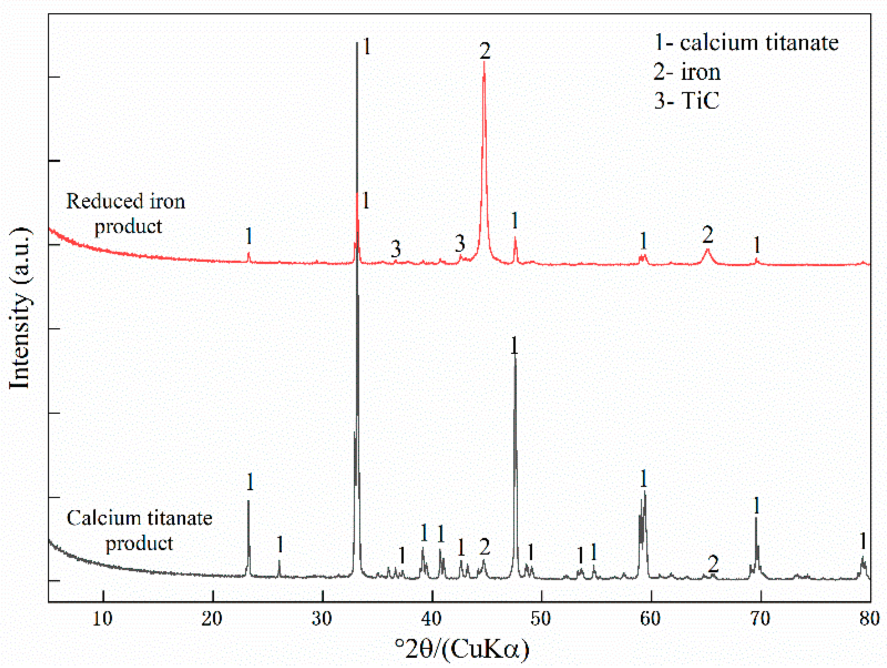

Figure 11. XRD analysis of reduced iron and calcium titanate products after magnetic separation.

Table 6. Rietveld results of magnetic separation products.

	R_{wp}	Calcium Titanate $CaTiO_3$	Fe	TiC	Magnetite
Reduced iron product (concentrate)	9.69	16.58 (3) *	78.05 (1)	3.19 (2)	1.28 (1)
Calcium titanate product (tailings)	8.36	90.87 (2)	4.78 (1)	1.35 (1)	-

*: the standard deviation.

4. Conclusions

In this study, calcium carbonate ($CaCO_3$) was used as an additive for the carbothermal reduction of ilmenite concentrate. Metallic iron and calcium titanate products were obtained through magnetic separation. The conclusions are as follows:

(1) The roasting temperature significantly influences the phase composition of the roasted products. With increasing temperature, calcium titanate ($CaTiO_3$) content rose from 21.95% to 83.02%. The addition of $CaCO_3$ is also crucial in calcium titanate formation, as Rietveld analysis showed that increasing $CaCO_3$ content led to a rise in calcium titanate from 0% to 83.11%. Calcium carbonate also promotes the reduction of metallic iron, as the metallic iron content in the reduction products increased from 4.52% to 10.37% with higher $CaCO_3$ content. SEM-EDS results further indicated that adding calcium carbonate in the carbothermic reduction of ilmenite encourages the aggregation and growth of metallic iron particles.

(2) The thermodynamic analysis results demonstrated that the standard Gibbs free energy of the chemical reaction was lower with the addition of calcium carbonate compared to without adding calcium carbonate. It indicated that adding calcium carbonate can facilitate the direct reduction of ilmenite, lower the reduction temperature, and make the process of reducing ilmenite to metallic iron more efficient.

(3) The roasted product, obtained under the optimal roasting conditions of 60% carbon dosage, 1400 °C roasting temperature, and 120 min roasting time, was subjected to three-stage grinding and three-stage magnetic separation. The final magnetic separation yielded a reduced iron product with a total iron grade of 90.01% and a recovery rate of 91.32%. The calcium titanate product contained 55.43% TiO_2, achieving a titanium recovery rate of 85.90%. Rietveld analysis results showed that the calcium titanate content in the tailings was 90.87%, while the iron content in the concentrate was 78.05%. This approach can effectively separate iron and titanium from ilmenite and produce calcium titanate with relatively high purity.

Supplementary Materials: The following supporting information can be downloaded at: https://www.mdpi.com/article/10.3390/met14121321/s1, Figure S1: title; Table S1: The Rietveld results of roasted products at different temperatures (lattice parameters). Table S2: The Rietveld results of roasted products with different amounts of calcium carbonate (lattice parameters). Figure S1: Structure model of calcium titanate (including atomic coordinates) during the Rietveld refinement. Figure S2: Structure model of iron (including atomic coordinates) during the Rietveld refinement. Figure S3: Structure model of Ferropseudobrookite (including atomic coordinates) during the Rietveld refinement.

Author Contributions: Conceptualization, X.W. and H.W.; methodology, investigation, data curation, X.W., Y.L., H.W. and C.S.; writing—original draft preparation, X.W. and Y.L.; writing—review and editing, X.W. and J.K.; supervision, H.W., C.S. and J.K.; project administration, X.W. and J.K.; funding acquisition, X.W. and J.K. All authors have read and agreed to the published version of the manuscript.

Funding: This research was funded by the Open Foundation of State Key Laboratory of Mineral Processing (grant no. BGRIMM-KJSKL-2022-22), Fundamental Research Funds for the Central Universities (grant no. FRF-TP-22-118A1), and the National Natural Science Foundation of China (grant no. 51674018).

Data Availability Statement: The raw data supporting the conclusions of this article will be made available by the authors on request.

Conflicts of Interest: The authors declare no conflicts of interest.

References

1. Buttner, R.H.; Maslen, E.N. Electron difference density and structural parameters in $CaTiO_3$. *Acta Crystallogr. Sect. B Struct. Sci.* **1992**, *48*, 644–649. [CrossRef]
2. AbdulKareem, S.K.; Ajeel, S.A. Effect of annealing temperatures on the structural and crystalline properties of $CaTiO_3$ powder synthesized via conventional solid-state method. *Mater. Today Proc.* **2021**, *42*, 2674–2679. [CrossRef]
3. Meng, L.; Yuan, C.; Liu, X.; Xu, J.; Liu, F.; Zhou, C.; Chen, G.; Wang, J. Electrical microstructures of $CaTiO_3$-$Bi_{0.5}Na_{0.5}TiO_3$ microwave ceramics with high permittivity ($\varepsilon_r{}^{max}$ ∼487). *J. Alloys Compd.* **2019**, *803*, 850–859. [CrossRef]
4. Patra, T.; Mohanty, A.; Muduli, S.; Parhi, P.K.; Sahoo, T. Effect of calcination temperature on morphology and phase transformation of MnO2 nanoparticles: A step towards green synthesis for reactive dye adsorption. *Chemosphere* **2021**, *288*, 132472. [CrossRef] [PubMed]
5. Clabel H, J.L.; Chacaliaza-Ricaldi, J.; Marega, E., Jr. Potential Application of Perovskite Structure for Water Treatment: Effects of Band Gap, Band Edges, and Lifetime of Charge Carrier for Photocatalysis. *Front. Nanotechnol.* **2022**, *4*, 827925. [CrossRef]
6. Mishra, S.; Naini, P.K.; Sundaram, B. Effect of calcination temperature on structural, optical and photocatalytic properties of calcium titanate ($CaTiO_3$) nanoparticle. *Results Opt.* **2024**, *16*, 100676. [CrossRef]
7. Heimann, R.B.; Lehmann, H.D. *Bioceramic Coatings for Medical Implants: Trends and Techniques*; John Wiley & Sons: Hoboken, NJ, USA, 2015.
8. Dubey, A.K.; Basu, B.; Balani, K.; Guo, R.; Bhalla, A.S. Multifunctionality of perovskites $BaTiO_3$ and $CaTiO_3$ in a composite with hydroxyapatite as orthopedic implant materials. *Integr. Ferroelectr.* **2011**, *131*, 119–126. [CrossRef]
9. Lin, N.; Gong, Y.; Wang, R.; Wang, Y.; Zhang, X. Critical review of perovskite-based materials in advanced oxidation system for wastewater treatment: Design, applications and mechanisms. *J. Hazard. Mater.* **2022**, *424*, 127637. [CrossRef]
10. Ferrari, A.M.; Germiniano, T.O.; Savoia, J.E.; Marques, R.G.; Ribeiro, V.A.; Ueda, A.C. $CaTiO_3$ Perovskite in the Photocatalysis of Textile Wastewater. *Rev. Ambiente Água* **2019**, *14*, 2336. [CrossRef]
11. Holliday, S.; Stanishevsky, A. Crystallization of $CaTiO_3$ by sol–gel synthesis and rapid thermal processing. *Surf. Coat. Technol.* **2004**, *188–189*, 741–744. [CrossRef]
12. Palaniandy, S.; Jamil, N.H. Influence of milling conditions on the mechanochemical synthesis of $CaTiO_3$ nanoparticles. *J. Alloys Compd.* **2009**, *476*, 894–902. [CrossRef]
13. Yang, J.; Zhang, L.; Wang, J.D.; Ji, J.N. Synthesis of calcium titanate by high temperature calcination with calcium hydroxide as calcium source. *Refractories* **2017**, *51*, 452.
14. Li, Z.H.; Wang, Z.C.; Li, G. Preparation of nano-titanium dioxide from ilmenite using sulfuric acid-decomposition by liquid phase method. *Powder Technol.* **2016**, *287*, 256–263. [CrossRef]
15. Yang, F.L.; Hlavacek, V. Effective extraction of titanium from rutile by a low-temperature chloride process. *AIChE J.* **2000**, *46*, 355–360. [CrossRef]
16. Song, Q.; Tsai, S.C. Flotation of ilmenite using benzyl arsonic acid and acidified sodium silicate. *Int. J. Miner. Process.* **1989**, *26*, 111–121. [CrossRef]
17. Mehdilo, A.; Irannajad, M.; Rezai, B. Chemical and mineralogical composition of ilmenite: Effects on physical and surface properties. *Miner. Eng.* **2015**, *70*, 64–76. [CrossRef]
18. Zhang, T.; Song, B. Research status of preparation of artificial rutile from iron and titanium by reduction grinding separation of ilmenite. *Light Metals.* **2020**, *502*, 42–44.
19. Zhang, Y.M.; Yi, L.Y.; Wang, L.N.; Chen, D.S.; Wang, W.J.; Liu, Y.H.; Zhao, H.X.; Qi, T. A novel process for the recovery of iron, titanium, and vanadium from vanadium-bearing titanomagnetite: Sodium modification–direct reduction coupled process. *Int. J. Miner. Metall. Mater.* **2017**, *24*, 504–511. [CrossRef]
20. Jiang, T.; Xu, J.; Guan, S.F.; Xue, X.X. Study on coalbased direct reduction of high-chromium vanadium-titanium magnetite. *J. Northeast. Univ. Nat. Sci.* **2015**, *36*, 77–81.
21. Zhao, Y.Q.; Sun, T.C.; Zhao, H.Y.; Chen, C.; Wang, X.P. Effect of reductant type on the embedding direct reduction of beach titanomagnetite concentrate. *Int. J. Miner. Metall. Mater.* **2019**, *26*, 152–159. [CrossRef]
22. Sarkar, B.K.; Samanta, S.; Dey, R.; Das, G.C. A study on reduction kinetics of titaniferous magnetite ore using lean grade coal. *Int. J. Miner. Process.* **2016**, *152*, 36–45. [CrossRef]
23. Li, X.; Kou, J.; Sun, T.; Guo, X.; Tian, Y. Coal and coke based reduction of vanadium titanomagenetite concentrate by the addition of calcium carbonate. *Miner. Process. Extr. Metall. Rev.* **2021**, *42*, 115–122. [CrossRef]
24. Li, X.; Kou, J.; Sun, T.; Wu, S.; Tian, Y. Effect of direct reduction time of vanadium titanomagnetite concentrate on the preparation and photocatalytic performance of calcium titanate. *Physicochem. Probl. Miner. Process.* **2021**, *57*, 75–86. [CrossRef]
25. Chen, C.; Sun, T.C.; Kou, J.; Zhao, Y.Q. Carbothermic reduction of vanadium titanomagnetite concentrate with magnesium compounds. *Rare Metals.* **2018**, *42*, 766–771.
26. Jung, S.M. Effects of $CaO/CaCO_3$ on the carbothermic reduction of titanomagnetite ores. *Metall. Mater. Trans. B* **2015**, *46*, 1162–1174. [CrossRef]
27. Li, X.H.; Kou, J.; Sun, T.C.; Wu, S.C.; Zhao, Y.Q. Effects of calcium compounds on the carbothermic reduction of vanadium titanomagnetite concentrate. *Int. J. Miner. Metall. Mater.* **2020**, *27*, 301–309. [CrossRef]
28. Chen, C.; Sun, T.C.; Wang, X.P.; Hu, T.Y. Effects of MgO on the reduction of vanadium titanomagnetite concentrates with char. *JOM* **2017**, *69*, 1759–1766. [CrossRef]

29. Yu, Z.D.; Xiao, J.W.; Leng, H.Y.; Chou, K.C. Direct carbothermic reduction of ilmenite concentrates by adding high dosage of Na_2CO_3 in microwave field. *Trans. Nonferrous Met. Soc. China* **2021**, *31*, 1818–1827. [CrossRef]
30. Rietveld, H.M. A profile refinement method for nuclear and magnetic structures. *J. Appl. Crystallogr.* **1969**, *2*, 65–71. [CrossRef]
31. Rietveld, H.M. Line profiles of neutron powder- diffraction peaks for structure refinement. *Acta Crystallogr.* **1967**, *22*, 151–152. [CrossRef]
32. Taut, T.; Kleeberg, R.; Bergmann, J. The new seifert Rieveld program BGMN and its application to quantitative phase analysis. *Mater. Struct.* **1998**, *5*, 57–66.
33. Bergmann, J.; Friedel, P.; Kleeberg, R. BGMN-a new fundamental parameters based Rietveld program for laboratory X-ray sources; it's use in quantitative analysis and structure investigations. *CPD Newsl.* **1998**, *20*, 5–8.
34. Hellenbrandt, M. The inorganic crystal structure database (ICSD)—Present and future. *Crystallogr. Rev.* **2004**, *10*, 17–22. [CrossRef]
35. Gražulis, S.; Daškevič, A.; Merkys, A.; Chateigner, D.; Lutterotti, L.; Quirós, M.; Serebryanaya, N.R.; Moeck, P.; Downs, R.T.A. Le Bail, Crystallography Open Database (COD): An open-access collection of crystal structures and platform for world-wide collaboration. *Nucleic Acids Res.* **2012**, *40*, 420–427. [CrossRef]
36. Li, X.H.; Kou, J.; Sun, T.C.; Wu, S.C.; Zhao, Y.Q. Formation of calcium titanate in the carbothermic reduction of vanadium titanomagnetite concentrate by adding $CaCO_3$. *Int. J. Miner. Metall. Mater.* **2020**, *27*, 745–753. [CrossRef]